AJNR

Effect of Age on MRI Phase Behavior in the Subcortical Deep Gray Matter of Healthy Individuals

J. Hagemeier, M.G. Dwyer, N. Bergsland, F. Schweser, C.R. Magnano, M. Heininen-Brown, D.P. Ramasamy, E. Carl, C. Kennedy, R. Melia, P. Polak, A. Deistung, J.J.G. Geurts, J.R. Reichenbach and R. Zivadinov

AJNR Am J Neuroradiol 2013, 34 (11) 2144-2151
doi: https://doi.org/10.3174/ajnr.A3569
http://www.ajnr.org/content/34/11/2144

Effect of Age on MRI Phase Behavior in the Subcortical Deep Gray Matter of Healthy Individuals

J. Hagemeier, M.G. Dwyer, N. Bergsland, F. Schweser, C.R. Magnano, M. Heininen-Brown, D.P. Ramasamy, E. Carl, C. Kennedy, R. Melia, P. Polak, A. Deistung, J.J.G. Geurts, J.R. Reichenbach, and R. Zivadinov

ABSTRACT

BACKGROUND AND PURPOSE: It has been demonstrated that increased levels of iron in the brain occur with aging. In this study we investigated the nature of the association between age and SWI-filtered phase values, indicative of iron content, in the subcortical deep gray matter of healthy individuals.

MATERIALS AND METHODS: A total of 210 healthy individuals (men: $n = 89$, women: $n = 121$), mean age, 39.8 years (standard deviation = 15.5; range = 6–76 years), were imaged on a 3T scanner. Mean MRI phase, mean phase of low-phase voxels, and normalized volumes were determined for total subcortical deep gray matter, caudate, putamen, globus pallidus, thalamus, pulvinar nucleus, hippocampus, amygdala, nucleus accumbens, red nucleus, and substantia nigra. Linear and nonlinear regression models were used to explore the relationship between phase and volume measures, and aging.

RESULTS: Mean phase values of subcortical deep gray matter structures showed a quadratic relationship, with individuals in late middle age (40–59 years) having the lowest mean phase values, followed by a reversal of this trend in the elderly. In contrast, mean phase of low-phase voxel measurements showed strong negative linear relationships with aging. Significantly lower phase values were detected in women compared with men ($P < .001$), whereas no sex differences were observed for mean phase of low-phase voxels. Normalized volume measurements were also linearly related to aging, and women showed smaller normalized volumes of subcortical deep gray matter structures than men ($P < .001$). Lower mean phase of low-phase voxels was related to decreased volume measures.

CONCLUSIONS: A strong association between phase (quadratic effect; phase decreases are followed by increases), mean phase of low-phase voxels (linear effect), volume (linear effect), and age was observed. Low phase was related to brain atrophy.

ABBREVIATIONS: SDGM = subcortical deep gray matter; MP-LPV = mean phase of low-phase voxels; NC = neocortex

For decades, changes in brain iron levels have been known to occur as a function of age.[1] Brain iron has been investigated in healthy individuals in both postmortem[1,2] and, more recently, in vivo studies with the use of different MR-based techniques.[3-11] Increased iron levels predominantly occur in brain subcortical deep gray matter (SDGM) structures such as the caudate, putamen, thalamus, red nucleus, and substantia nigra. Furthermore, it has been found that brain iron accumulation is influenced by sex.[3,12-14] Extensive increases in brain iron content occur in neurodegenerative disorders such as Alzheimer disease,[15] Parkinson disease,[16] Huntington disease,[17] and Friedreich ataxia.[18] Most of these disorders have a disease onset at or after middle age (40–59 years). Brain iron accumulation is currently discussed as a contributing, modulating, and even initiating factor in the development of neurodegenerative and neuroinflammatory disorders such as multiple sclerosis,[19] because of its neurotoxic effects caused by free radical generation.[20]

Several MRI techniques allow for the in vivo imaging of paramagnetic substances such as iron in the brain. In this study, we used SWI-filtered phase imaging.[21] This technique takes advantage of magnetic field changes caused by substances such as iron or ferritin through their influences on the phase of the proton spin.[21,22] Although it does have nonlocal dipole field effects that can potentially be alleviated by susceptibility mapping, it involves fewer

Received December 26, 2012; accepted after revision February 12, 2013.

From the Buffalo Neuroimaging Analysis Center (J.H., M.G.D., N.B., C.R.M., M.H.-B., D.P.R., E.C., C.K., R.M., P.P., R.Z.), Department of Neurology, University at Buffalo, Buffalo, New York; Medical Physics Group (F.S., A.D., J.R.R.), Institute of Diagnostic and Interventional Radiology I, Jena University Hospital–Friedrich Schiller University, Jena, Germany; and Department of Anatomy and Neurosciences (J.J.G.G.), Section of Clinical Neuroscience, VU University Medical Center, Amsterdam, The Netherlands.

Please address correspondence to Robert Zivadinov, MD, PhD, FAAN, Department of Neurology, School of Medicine and Biomedical Sciences, Buffalo Neuroimaging Analysis Center, 100 High St, Buffalo, NY 14203; e-mail: zivadinov@hotmail.com

Indicates open access to non-subscribers at www.ajnr.org

Indicates article with supplemental on-line figures.

http://dx.doi.org/10.3174/ajnr.A3569

Table 1: Demographic characteristics and global volumetric MRI measures of study participants

	Total	Male	Female	*P*
n (%)	210	89 (42.4)	121 (57.6)	
Age (SD) median	39.8 (15.5) 41	38 (16.1) 38	41.1 (14.9) 44	.202
Race, *n* (%) of available cases				
White	139 (87.4)	58 (87.9)	81 (87.1)	.617
African American	13 (8.2)	5 (7.6)	8 (8.6)	
Other	7 (4.4)	3 (4.5)	4 (4.3)	
Education, *n* (%) of available cases				
No high school	15 (9.7)	7 (11.3)	8 (8.7)	.893
High school	24 (15.6)	11 (17.7)	13 (14.1)	
Some college	32 (20.8)	14 (22.6)	18 (19.6)	
Associate/technical	22 (14.3)	7 (11.3)	15 (16.3)	
Bachelor level	36 (23.4)	12 (19.4)	24 (26.1)	
Graduate level	23 (14.9)	10 (16.1)	13 (14.1)	
Postgraduate	2 (1.3)	1 (1.6)	1 (1.1)	
MRI volumes in cm^3, mean (SD)				
WM hyperintensities	1.26 (4.47)	1.74 (6.50)	0.87 (1.29)	.160
GM	791.93 (65.56)	787.64 (69.36)	795.02 (62.81)	.525
Cortical GM	644.30 (56.33)	637.10 (62.11)	649.56 (51.36)	.181
WM	761.95 (41.39)	771.66 (39.57)	754.97 (41.41)	.008
Lateral ventricles	31.66 (12.70)	33.46 (13.36)	30.35 (12.07)	.136

Note:—Differences between men and women were assessed by means of the χ^2 test (race and education) and Student *t* test (age and normalized volumes).

assumptions caused by the ill-posed problem of dipole de-convolution, is still widely used by researchers, and is more generally applicable because it is directly available on some scanners. Furthermore, both post-mortem[23-26] and in vivo [27] studies confirmed associations between the local SWI-filtered phase shift and the underlying magnetic susceptibility, which is affected by the tissue iron content. In the present study, both mean phase (indicative of overall iron content) and mean phase of low-phase voxels (MP-LPV) (indicative of high iron content) measures were used. Recent work has shown strong correlations between SDGM MP-LPV measurements and brain volume reductions in patients with multiple sclerosis.[19]

In the present study, we sought to investigate age- and sex-dependent changes in SWI-filtered phase in healthy individuals by assessing mean phase, MP-LPV, and volumetric measures. Age-associated patterns of these MR imaging measures were investigated on a structure-by-structure basis. Furthermore, the relationship between SWI-filtered phase and structural volumes was explored.

MATERIALS AND METHODS

Subjects

A total of 210 volunteers without known CNS pathology (men: $n = 89$, women: $n = 121$) were recruited from community and hospital staff. Inclusion criteria for this study were fulfilling health screen questionnaire requirements containing information about medical history (illnesses, surgeries, medications, etc) or physical examination and being capable of undergoing a diagnostic examination with MR imaging. Exclusion criteria were pre-existing medical conditions known to be associated with CNS pathology. Age of the participants ranged between 6–76 years (mean = 39.8 years, standard deviation [SD] = 15.5 years, median = 41, interquartile range = 24.3). Demographic characteristics of the subjects are shown in Table 1.

The study protocol was approved by the local institutional review board, and all participants provided their written informed consent before examination.

Image Acquisition

All scans were carried out on a 3T Signa Excite HD 12.0 scanner (GE Healthcare, Milwaukee, Wisconsin), with the use of a multi-channel head and neck coil. SWI was acquired by use of a 3D flow-compensated gradient-echo sequence with 64 sections, 2-mm section thickness, FOV = 25.6 cm × 19.2 cm, and in-plane resolution of 0.5 mm × 1 mm (flip angle = 12°; TE/TR = 22/40 ms; acquisition time = 8:46 min:s; bandwidth = 13.89 kHz).[19]

Additional 2D sequences were acquired by use of a 256 × 192 matrix (frequency × phase), 25.6 cm × 19.2 cm FOV, resulting in an in-plane resolution of 1 mm × 1 mm, with 48 gapless 3-mm sections for whole-brain coverage. Sequence-specific parameters were dual FSE proton attenuation and T2WI (TE1/TE2/TR = 9 /98/5300 ms; echo-train length = 14); FLAIR (TE/TI/TR = 120/2100/8500 ms; flip angle = 90°; echo-train length = 24); and spin-echo T1WI (TE/TR = 16/600 ms). Moreover, a 3D high-resolution T1WI fast spoiled gradient-echo sequence with a magnetization-prepared inversion recovery pulse was acquired (TE/TI/TR = 2.8/900/5.9 ms, flip angle = 10°) by use of 184 locations 1 mm thick, resulting in isotropic resolution.

All scans were prescribed parallel to the subcallosal line in an axial-oblique orientation, and no averaging was performed.

Image Analyses

Mean and Low Mean Phase Identification. Segmentation of SDGM structures for volumetric and SWI analysis was performed by use of the FMRIB Software Library's integrated registration and segmentation tool (FIRST; http://www.fmrib.ox.ac.uk/fsldownloads/) on the 3D T1WI.[28] Additional structures not identifiable this way (red nucleus, pulvinar nucleus, and substantia nigra) were manually delineated on the most representative section by a single operator (M.H.-B.) with the use of JIM5 (Xinapse Systems Ltd, Northamptonshire, United Kingdom), as reported previously.[29]

An overview of the SWI processing, analysis method, and reproducibility results used in the present study is discussed elsewhere.[19] In this study, the MP-LPV of each structure was determined by thresholding the phase images to retain only those voxels with phase values lower than 2 SD below the reference group means, as explained elsewhere.[19,30] However, for the present study, normal reference phase values (both means and SDs) for each structure were determined on a group of 330 healthy control subjects distributed in age groups ranging from 8–87 years who obtained their SWI scans on the same scanner. The volumes of thresholded voxels were subsequently used to compute the proportion of low-phase voxels versus normalized volume, on a structure-by-structure basis. As a measure of the degree

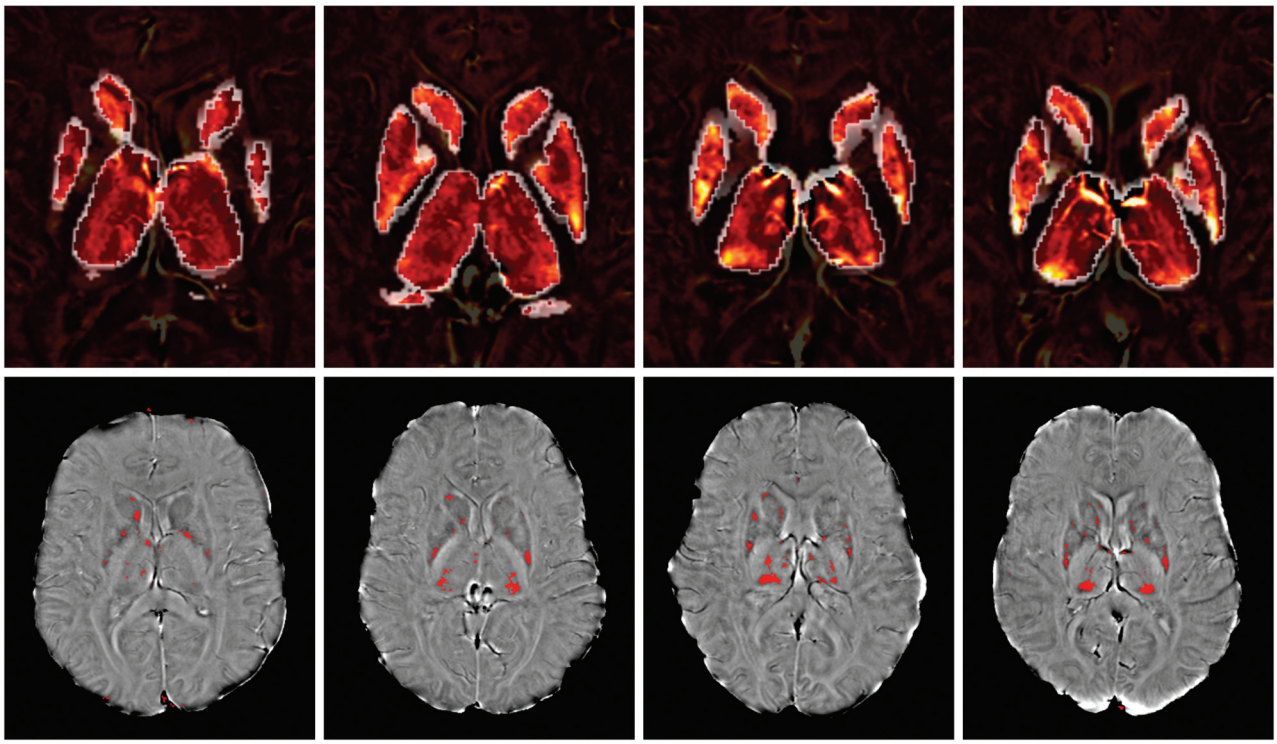

FIG 1. Phase maps (*upper row*) and thresholded low-phase voxels used in mean phase of low-phase voxel (MP-LPV) calculation (*bottom row*) of subcortical deep gray matter structures. MP-LPV was determined by thresholding the phase images to retain only those voxels with phase values lower than 2 standard deviations below reference group. Upper and lower rows show the same subjects, and each column contains a representative subject from each age group (left to right, <25 years, 25–39 years, 40–55 years, >55 years).

of phase abnormality, the mean phase values of the resulting thresholded voxels were calculated, yielding MP-LPV (Fig 1). Structure-specific maps of voxels with phase and low phase are presented in radians, with lower phase and MP-LPV values suggesting increased iron content.

Global Volumetric and WM Hyperintensity Analyses. SIENAX version 2.6 in FSL (http://www.fmrib.ox.ac.uk/fsl/feeds/doc/index.html) was used for brain extraction and tissue segmentation on 3D T1WI.[19] Normalized volume measures of the whole brain, GM, neocortex (NC), WM, and lateral ventricles were acquired.[31] WM hyperintensity volumes were calculated by means of a semi-automated edge-detection contouring-thresholding technique, as previously described.[19]

Statistical Analysis

All analyses were carried out by use of IBM SPSS Statistics 20 (IBM Corp, Armonk, New York). Demographic and sex differences of mean phase, MP-LPV, and normalized volumes were assessed by means of independent-samples *t* test and the Mann-Whitney *U* test, as well as the χ^2 test, where appropriate.

Linear regression models were fitted on the data, adjusting for the effects of sex. Models of mean phase and MP-LPV were also adjusted for normalized structural volume to reduce the confounding effects atrophy may have on phase shift. After this, it was determined whether a quadratic regression function yielded a more reasonable fit than a linear slope by assessing the change in R^2 between the models and determining statistical significance by means of an *F* test. This allowed us to determine the relationship between structural mean phase, MP-LPV, and normalized volumes with aging in both linear, and, when applicable, nonlinear models. Interaction terms between sex and age were added to the models to assess sex differences, as a function of age. Additional general linear models were computed to assess whether the relative volume of structural low phase tissue versus total structural volume differs among age groups.

To evaluate the association between mean phase and MP-LPV measurements with volumes, we used Spearman rank correlations. The Benjamini-Hochberg correction at the $P < .05$ level was used to minimize the false discovery rate.[32]

RESULTS

No significant differences were observed between men and women regarding demographic or global volumetric MRI characteristics (Table 1).

Sex Differences

Table 2 lists mean phase, MP-LPV, and normalized volumes for SDGM structures, according to sex. Normalized WM volume was smaller among women ($P = .008$, Table 1). Significantly lower phase values were detected in women compared with men in the caudate ($P < .001$). Phase values in the total SDGM and putamen were also lower among women. No sex differences were observed in MP-LPV, whereas normalized volumes of most SDGM structures were significantly smaller among women than men (Table 2).

Age-Dependent Effects

Because sex differences were observed (Table 2), initial linear regression models included sex as a covariate (Table 3). A decrease

Table 2: Sex differences of mean phase, mean phase of low-phase voxels, and normalized volume values of subcortical deep gray matter structures

	Mean Phase			MP-LPV			Normalized Volume		
	Male (n = 89)	Female (n = 121)	P	Male (n = 89)	Female (n = 121)	P	Male (n = 89)	Female (n = 121)	P
Total SDGM	−.012 (.014)	−.016 (.014)	.036	−.144 (.022)	−.149 (.027)	.573	49.209 (5.474)	44.442 (3.551)	<.001
Caudate	−.054 (.017)	−.064 (.018)	.001	−.170 (.016)	−.167 (.014)	.525	7.398 (1.079)	6.832 (.890)	<.001
Putamen	−.018 (.028)	−.027 (.029)	.028	−.175 (.039)	−.183 (.047)	.487	10.471 (1.386)	9.426 (.914)	<.001
Globus pallidus	−.016 (.025)	−.015 (.024)	.643	−.184 (.033)	−.183 (.042)	.348	3.809 (.442)	3.431 (.399)	<.001
Thalamus	.005 (.008)	.003 (.009)	.210	−.095 (.015)	−.091 (.013)	.157	16.474 (1.923)	14.661 (1.188)	<.001
Pulvinar	−.042 (.030)	−.042 (.028)	.657	−.139 (.017)	−.140 (.018)	.689	.456 (.092)	.419 (.090)	.010
Hippocampus	.024 (.032)	.031 (.039)	.073	−.161 (.044)	−.165 (.049)	.822	7.559 (.956)	6.981 (.817)	<.001
Amygdala	.011 (.039)	−.007 (.066)	.086	−.214 (.051)	−.210 (.075)	.086	2.634 (.424)	2.326 (.307)	<.001
Accumbens	−.179 (.140)	−.230 (.163)	.035	−.744 (.203)	−.80 (.252)	.298	.865 (.199)	.784 (.189)	.006
Red nucleus	−.050 (.057)	−.059 (.051)	.331	−.238 (.027)	−.232 (.026)	.225	.179 (.023)	.162 (.022)	<.001
Substantia nigra	−.097 (.056)	−.096 (.057)	.765	−.305 (.039)	−.308 (.041)	.574	.305 (.048)	.282 (.053)	.005

Note:—Results are shown as mean (standard deviation); volume measurements are expressed in cubic centimeters. Mean phase and mean phase of low-phase tissue (MP-LPV) measurements are expressed in radians. Statistical analyses were carried out by use of independent-samples t test and Mann-Whitney U test.

Table 3: Linear regression analyses assessing the association between age and mean phase, mean phase of low-phase tissue, and normalized volumes, adjusted for sex

	Mean phase[a]		MP-LPV[a]		Normalized Volume	
	β	P	β	P	β	P
Total SDGM	−.102	.057	−.255	<.001	−.245	<.001
Caudate	−.102	.068	−.350	<.001	−.247	<.001
Putamen	−.208	<.001	−.193	<.001	−.239	<.001
lobus pallidus	.210	<.001	−.273	<.001	.049	.352
Thalamus	−.178	<.001	−.521	<.001	−.299	<.001
Pulvinar nucleus	−.384	<.001	−.340	<.001	−.105	.059
Hippocampus	−.027	.645	.033	.589	−.075	.163
Amygdala	.039	.525	−.029	.631	.069	.197
Accumbens	−.051	.376	.112	.043	−.271	<.001
Red nucleus	−.301	<.001	−.252	<.001	−.195	<.001
Substantia nigra	−.207	.006	−.256	<.001	.023	.687

[a] Adjusted for the effects of normalized volume.

in mean phase values in the red nucleus, pulvinar nucleus, putamen, and thalamus, as well as an increase in mean phase values in the globus pallidus, were strongly related with increasing age ($P <$ .001). The strongest associations with age were observed in MP-LPV measurements of the caudate, pulvinar nucleus, total SDGM, substantia nigra, globus pallidus, red nucleus, and putamen ($P <$ .001). The association of age and thalamus MP-LPV was particularly strong ($\beta = -.521$, $P < .001$). Thalamus, nucleus accumbens, caudate, total SDGM, putamen, and red nucleus normalized volumes were inversely related to aging ($P < .001$). There was also an interaction effect of sex for both putamen mean phase and MP-LPV ($P = .010$) and substantia nigra MP-LPV ($P = .003$) (Fig 2).

Fitting of curved regression lines was conducted to determine whether the association between MR imaging measurements and age were better represented by nonlinear slopes. The linear and quadratic effects, as determined by R^2 fit parameters, of the association between age and representative SDGM structure mean phase, MP-LPV, and normalized volume are represented in Online Figs 1 and 2. Regression line fits for each structure were similar for both sexes. The relationship between age and mean phase of the total SDGM ($R^2 = 0.055$, $F = 11.96$), caudate ($R^2 = 0.087$, $F = 19.25$), thalamus ($R^2 = 0.126$, $F = 29.26$), pulvinar nucleus ($R^2 = 0.161$, $F = 38.85$), and red nucleus ($R^2 = 0.240$, $F = 63.90$) were significantly quadratically related to aging ($P < .001$), with individuals in late middle age having the lowest mean phase values followed by a reversal of this trend in the elderly. Associations between age and the mean phase of the putamen, globus pallidus, hippocampus, amygdala, nucleus accumbens, and substantia nigra were best explained by linear slopes. MP-LPV measurements showed strong linear relationships with age, with only the red nucleus having a quadratic effect ($R^2 = 0.123$, $F = 24.63$, $P <$ .001). Normalized volume measurements were not quadratically related to aging.

The relative size of structural low-phase tissue volume versus normalized structural volume was also investigated (Table 4) to assess whether a greater proportion of a given SDGM structure can be considered to consist of low-phase voxels after thresholding. Older patients had a significantly higher proportion of MP-LPV volume in the total SDGM, caudate, putamen, thalamus, pulvinar nucleus, red nucleus (all $P < .001$), and substantia nigra ($P = .002$). In contrast, the proportion of MP-LPV volume decreased in the globus pallidus as a function of age ($P < .001$). There was no effect of sex on the proportion of MP-LPV volume.

Relationship Between Iron and Volumetric MRI Outcomes

We used Spearman rank correlations to assess the relationship between mean phase and MP-LPV measurements and brain volumetric measures. Associations were observed between normalized GM and NC volume with mean phase values of the total SDGM, caudate, putamen, thalamus, hippocampus, and red nucleus ($r = .139$–$.272$, $P < .01$) and inversely with the globus pallidus ($r = -.226$ to $-.232$, $P < .001$). The strongest associations of mean phase measurements were observed in the pulvinar nucleus with normalized GM ($r = 0.387$, $P < .001$), lateral ventricle ($r = -.234$, $P < .001$), and NC ($r = 0.399$, $P <$ .001) volumes.

Associations ($P < .001$) were also observed between the MP-LPV measurements of the total SDGM, caudate, putamen, globus pallidus, and thalamus with GM, lateral ventricle, and NC volumes, with the strongest correlations occurring between thalamic MP-LPV and normalized GM ($r = .487$, $P < .001$), lateral ventricle ($r = -.376$, $P < .001$), and NC volumes ($r = .472$, $P < .001$). Correlations of MP-LPV measurements with WM volume were less robust ($r = .105$–$.171$, $P < .05$).

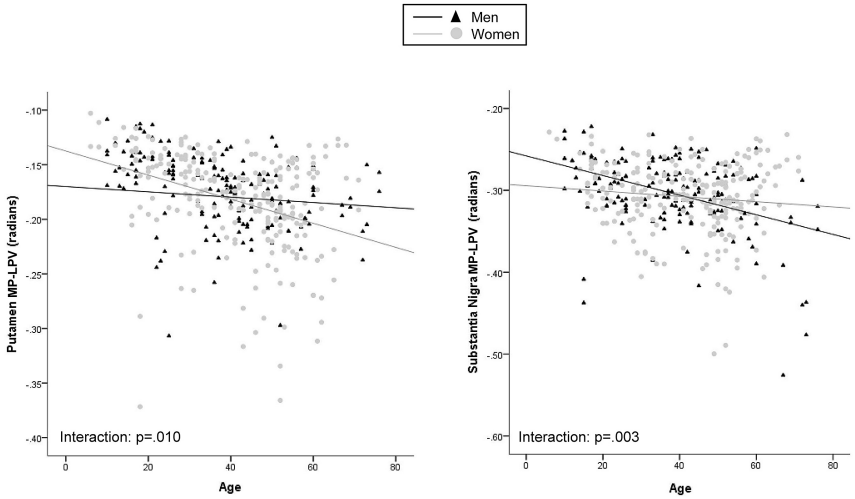

FIG 2. Scatterplots showing significant interaction effects between sex and the mean phase of low-phase voxels (MP-LPV) of the putamen and substantia nigra.

Table 4: Proportion of structural low-phase voxels versus structural normalized volume within age groups, adjusted for sex

	Age (years)				
	<25 *n* = 43	25–39 *n* = 56	40–55 *n* = 72	≥55 *n* = 39	*P*
Total SDGM	.29 (.04)	.32 (.03)	.34 (.04)	.35 (.04)	<.001
Caudate	.27 (.09)	.33 (.08)	.36 (.07)	.35 (.08)	<.001
Putamen	.17 (.08)	.26 (.06)	.33 (.07)	.32 (.09)	<.001
Globus pallidus	.42 (.07)	.40 (.06)	.38 (.06)	.35 (.06)	<.001
Thalamus	.40 (.03)	.43 (.03)	.44 (.04)	.43 (.04)	<.001
Pulvinar nucleus	.11 (.08)	.24 (.16)	.28 (.15)	.29 (.14)	<.001
Hippocampus	.15 (.08)	.19 (.09)	.18 (.07)	.18 (.07)	.319
Amygdala	.17 (.14)	.18 (.10)	.17 (.10)	.16 (.08)	.738
Accumbens	.15 (.14)	.14 (.14)	.12 (.13)	.13 (.16)	.703
Red nucleus	.05 (.05)	.13 (.12)	.21 (.13)	.17 (.11)	<.001
Substantia nigra	.17 (.11)	.23 (.11)	.27 (.11)	.24 (.14)	.002

General linear modeling comparing the proportion of structural low-phase voxels versus structural normalized volume between age groups. Results are presented as mean (standard deviation).

DISCUSSION

In the present study, we aimed to investigate the relationship between aging and SWI-filtered phase measures in the SDGM of healthy individuals. The aging behavior of total mean phase and the mean phase of low-phase voxels, which are indicative of brain iron levels, were assessed in a large cohort of healthy individuals. After adjusting for confounders, strong associations were observed between SDGM structure mean phase, MP-LPV, and normalized volumes with age, corroborating previous findings that brain iron content increases when a person ages.[1,3,6,10,33] Interestingly, strong correlations were observed especially between the MP-LPV and brain volume.

In this study, we used the SWI-filtered phase imaging method, which has been proposed as a method to indirectly measure iron content. MP-LPV was used as a measure of the level of high iron content and its volume, because only the mean phase values of the most severely affected voxels are measured, as previously determined by assessing only voxels with phase values more than 2 SD from the mean.[19,30] On the basis of the examined structures, the proportion of these voxels ranged from 5% in the red nucleus in age group <25 years to 44% in the thalamus in age group 40–55 years.

Sex Phase Differences

As indicated by interaction effects, women had a slightly higher rate of decrease in mean phase and MP-LPV over time in the putamen, whereas men showed a more steady decrease of substantia nigra MP-LPV as a function of age. This suggests that among women, MP-LPV increases at a more rapid pace in the putamen, whereas in men the substantia nigra has an accelerated rate. Previous MR imaging findings reported decreased brain iron levels among women in the caudate, thalamus, and several WM regions.[12] However, Xu et al[3] did not observe any significant sex differences by use of SWI. We suspect that sex differences are present on a minor level, and these became detectable because of our sizeable sample.[34-37] Future studies should further elucidate the relationship between sex-specific factors possibly influencing MR imaging phase (menses, child birth, hysterectomy, etc).

Aging Phase Behavior

Regression analyses showed strong associations between SWI-filtered phase measurements of the putamen, thalamus, red nucleus, and pulvinar nucleus with age, confirming previous findings.[1,6,9,33] However, mean phase measures of the total SDGM, caudate, hippocampus, amygdala, and nucleus accumbens were not significantly associated with aging. In addition, we did not observe an association between hippocampus mean phase and age, which is in contrast to a recent study in which a linear dependence was observed between hippocampal T2* and age.[8] Interestingly, the globus pallidus showed an inverse relationship of age with mean phase, suggesting that in this structure, the overall phase increases over time. This finding is in contrast to previous histologic publications[1] and may be due to the effect of the relatively high myelin content of the structure on MR imaging phase[38] or the presence of diamagnetic substances (eg, calcium) in elderly subjects.[39] However, a recent phase-imaging study also found slightly increased phase in older subjects.[3] Overall, the strongest associations were observed in MP-LPV measures, in which thalamic MP-LPV showed a particularly strong association with age. Although these and several previous[1,40] results implicate the thalamus, a recent study only found caudate and putamen but not thalamus relaxation rates to be increased with age.[41] This may be explained by the overall lower iron content of this structure,[1] making it more difficult to detect small age-related changes with the use of less sensitive MR imaging techniques.

In addition to finding significant linear relationships, when examining individual structure scatterplots, distinct age-dependent patterns were observed. Mean phase measures increased with age until early middle age and then tended to level off, some-

thing which was observed histopathologically in 1958.[1] Most studies have also shown either early-life MR imaging changes suggestive of increased iron, followed by flattening of the curve at later ages, or have reported linearly increasing effects.[3,7,10,11,33,41] In several structures, such as the caudate, putamen, thalamus, pulvinar nucleus, red nucleus, and substantia nigra, we observed slight reversions of the phase values after approximately 50 years of age. In fact, in several of the largest SDGM structures, a quadratic line fit was better than a linear one, including the caudate, thalamus, and pulvinar nucleus. This is a departure from conventional thinking that iron levels increase or level off with age. It appears that a decrease in iron content in older age is not confined to the thalamus, a phenomenon that was observed by Hallgren and Sourander,[1] but that also basal ganglia and red nucleus mean phase levels slightly increase again in the elderly after observing marked decreases before middle age. In contrast to these nonlinear findings of mean phase measures versus age, MP-LPV measures increased linearly with age in most investigated structures, with the exception of the hippocampus, amygdala, and nucleus accumbens, which did not show any notable upward or downward trend over time, and the red nucleus, which showed a curved relationship. A strong, strictly linear increase over time in MP-LPV indicates that high iron content accumulates continuously among the elderly, in contrast to mean phase measurements. In a recent study,[40] through the use of manually segmented SDGM structures, it was shown that not only did measures of high iron-content brain structures increase continuously with time, it appeared to accelerate with age. In the present study, we used automatically segmented SDGM structures, and the decrease in MP-LPV corresponded strikingly with decreases in normalized volumes in the corresponding structures. This suggests that there is an association between the mean phase of severely affected tissues and structural atrophy, though it is unknown at this time which of these observations, if any, is causative. Furthermore, with the exception of the globus pallidus, the volume of low-phase voxels (with <2 SD mean phase levels) encompasses a greater proportion of the corresponding SDGM structure volume in older subjects. This suggests that a larger percentage of SDGM structures is considered to consist of low-phase voxels. In neurodegenerative disorders in which increased iron content is observed, the age of onset is at or after middle age. Considering that mean phase measures tend to reverse in the elderly but that the MP-LPV continuously decreases with age would suggest that it is the severely affected tissues that are potentially related to neurodegenerative disease pathology.

Different aging behavior between mean phase and MP-LPV may have important implications for conducting longitudinal clinical trials in which measurement of iron content is one of the primary outcomes of the study. Linear increase of the MP-LPV with aging, as evidenced in the present study, may make this measure more suitable for use in longitudinal trials of patients affected by neurodegenerative disorders than mean phase, which showed quadratic behavior.

Phase and Atrophy

Modest to strong relationships were found between SDGM mean phase and MP-LPV measurements and reductions of the global brain volumes, such as reductions in the volume of the GM and NC, or increases in ventricular size. The SDGM structure showing the most prominent association with GM loss was the thalamus. The strong correlation of the thalamic MP-LPV with GM volume loss is an intriguing finding, suggesting that these 2 separate observations may be intricately related. The thalamus has a plethora of cortical and subcortical connections throughout the brain,[42,43] and it is therefore reasonable that local pathology has widespread consequences. However, whether increased iron content is causally related to such volume loss, an effect of it, or both remains to be determined.

Even though mean phase values increased in the globus pallidus, MP-LPV values decreased, the normalized volume remained constant over time, and there was a reduction in the relative amount of low-phase voxels. This suggests that unlike other brain structures in which MP-LPV and volume loss were strongly related, in this particular structure, focal phase shifts were not associated with an increased loss of corresponding tissue. Also, in the pulvinar nucleus and substantia nigra, decreases in MP-LPV values were observed without corresponding structural atrophy. This indicates that these particular phase effects are likely to be caused exclusively by increased iron content, because atrophy effects could not have strongly influenced the phase measurements. Perhaps even more interesting, there were strong correlations of several brain structure mean phase (hippocampus and pulvinar) and MP-LPV (globus pallidus) findings with lateral ventricles, GM, and NC atrophy, even though there was no structural volume loss in the corresponding SDGM structures as determined by regression analyses. This, together with the strong findings in the thalamus, may suggest that independent of any age effects, pathology observed in SWI-filtered phase is related to widespread damage even in the absence of structure-specific damage.

Limitations and Implications

Paramagnetic substances, mostly in the form of ferritin and iron, influence the phase of proton spin. It is unlikely, yet it remains possible, that other paramagnetic substances influence MR imaging phase measures, considering that these substances are not present in high enough concentrations.[44] Even though mean phase measures are probably caused by iron, phase shifts could potentially also be caused by other factors,[23,24,27,45] for example, by the diamagnetic properties of myelin.[27] In the present study, only GM structures were investigated, minimizing the confounding effects of myelin, which would be of greater concern if studying WM.[38] However, it must noted that some SDGM structures, most notably the thalamus, have relatively high myelin content, which could potentially have influenced phase measurements. Mean phase changes could also be influenced by atrophy or high-pass filtering effects.[27] However, this potential effect was limited by adding normalized volume to the regression models as a confounding factor to adjust for such structural atrophy effects influencing phase measures. In addition, findings from the present study largely replicate previous postmortem histopathologic findings.[1,2] SWI-filtered phase imaging is an in vivo method; therefore, all values are merely indirect measurements of iron levels. Furthermore, this was a cross-sectional study with all its inherent limitations, and longitudinal confirmation is needed. Because

most neurodegenerative disorders are linked to both age and brain iron deposition, and increased brain iron levels have detrimental effects through the generation of free radicals,[46] it is crucial to fully understand the relationship between increased brain iron levels in healthy individuals and their potential relationship with brain disorders through the use of different MR imaging techniques sensitive to paramagnetic substances.

CONCLUSIONS

The present study shows both linear (MP-LPV) and quadratic (mean phase) effects in healthy individuals by use of SWI-filtered phase imaging. In addition, decreased MP-LPV in the SDGM was shown to be strongly related to global brain atrophy.

ACKNOWLEDGMENTS

The authors thank Eve Salczynski for technical assistance in the preparation of the manuscript.

Disclosures: Robert Zivadinov—*UNRELATED: Consultancy* and *Payment for Lectures (including service on speakers bureaus):* Biogen Idec, EMD Serono, Teva Pharmaceuticals, Genzyme-Sanofi, Novartis; *Grants/Grants Pending:* Biogen Idec, EMD Serono, Teva Pharmaceuticals, Genzyme-Sanofi. Jeroen Geurts—*UNRELATED: Consultancy:* Merck Serono, Biogen Idec, Teva Pharmaceuticals.

REFERENCES

1. Hallgren B, Sourander P. **The effect of age on the non-haemin iron in the human brain.** *J Neurochem* 1958;3:41–51
2. Connor JR, Snyder BS, Beard JL, et al. **Regional distribution of iron and iron-regulatory proteins in the brain in aging and Alzheimer's disease.** *J Neurosci Res* 1992;31:327–35
3. Xu X, Wang Q, Zhang M. **Age, gender, and hemispheric differences in iron deposition in the human brain: an in vivo MRI study.** *Neuroimage* 2008;40:35–42
4. Thomas LO, Boyko OB, Anthony DC, et al. **MR detection of brain iron.** *AJNR Am J Neuroradiol* 1993;14:1043–48
5. Pfefferbaum A, Adalsteinsson E, Rohlfing T, et al. **MRI estimates of brain iron concentration in normal aging: comparison of field-dependent (FDRI) and phase (SWI) methods.** *Neuroimage* 2009;47:493–500
6. Bartzokis G, Beckson M, Hance DB, et al. **MR evaluation of age-related increase of brain iron in young adult and older normal males.** *Magn Reson Imaging* 1997;15:29–35
7. Adisetiyo V, Jensen JH, Ramani A, et al. **In vivo assessment of age-related brain iron differences by magnetic field correlation imaging.** *J Magn Reson Imaging* 2012;36:322–31
8. Rodrigue KM, Haacke EM, Raz N. **Differential effects of age and history of hypertension on regional brain volumes and iron.** *Neuroimage* 2011;54:750–59
9. Bilgic B, Pfefferbaum A, Rohlfing T, et al. **MRI estimates of brain iron concentration in normal aging using quantitative susceptibility mapping.** *Neuroimage* 2012;59:2625–35
10. Schenker C, Meier D, Wichmann W, et al. **Age distribution and iron dependency of the T2 relaxation time in the globus pallidus and putamen.** *Neuroradiology* 1993;35:119–24
11. Hardy PA, Gash D, Yokel R, et al. **Correlation of R2 with total iron concentration in the brains of rhesus monkeys.** *J Magn Reson Imaging* 2005;21:118–27
12. Bartzokis G, Tishler TA, Lu PH, et al. **Brain ferritin iron may influence age- and gender-related risks of neurodegeneration.** *Neurobiol Aging* 2007;28:414–23
13. Tishler TA, Raven EP, Lu PH, et al. **Premenopausal hysterectomy is associated with increased brain ferritin iron.** *Neurobiol Aging* 2012;33:1950–58
14. Bartzokis G, Tishler TA, Shin IS, et al. **Brain ferritin iron as a risk factor for age at onset in neurodegenerative diseases.** *Ann N Y Acad Sci* 2004;1012:224–36
15. Bartzokis G, Sultzer D, Mintz J, et al. **In vivo evaluation of brain iron in Alzheimer's disease and normal subjects using MRI.** *Biol Psychiatry* 1994;35:480–87
16. Sian-Hulsmann J, Mandel S, Youdim MB, et al. **The relevance of iron in the pathogenesis of Parkinson's disease.** *J Neurochem* 2011;118:939–57
17. Bartzokis G, Tishler TA. **MRI evaluation of basal ganglia ferritin iron and neurotoxicity in Alzheimer's and Huntington's disease.** *Cell Mol Biol* 2000;46:821–33
18. Waldvogel D, van Gelderen P, Hallett M. **Increased iron in the dentate nucleus of patients with Friedrich's ataxia.** *Ann Neurol* 1999;46:123–25
19. Zivadinov R, Heininen-Brown M, Schirda CV, et al. **Abnormal subcortical deep-gray matter susceptibility-weighted imaging filtered phase measurements in patients with multiple sclerosis: a case-control study.** *Neuroimage* 2012;59:331–39
20. Jomova K, Valko M. **Advances in metal-induced oxidative stress and human disease.** *Toxicology* 2011;283:65–87
21. Haacke EM, Xu Y, Cheng YC, et al. **Susceptibility weighted imaging (SWI).** *Magn Reson Med* 2004;52:612–18
22. Haacke EM, Cheng NY, House MJ, et al. **Imaging iron stores in the brain using magnetic resonance imaging.** *Magn Reson Imaging* 2005;23:1–25
23. Bagnato F, Hametner S, Yao B, et al. **Tracking iron in multiple sclerosis: a combined imaging and histopathological study at 7 Tesla.** *Brain* 2011;134(Pt 12):3602–15
24. Yao B, Bagnato F, Matsuura E, et al. **Chronic multiple sclerosis lesions: characterization with high-field-strength MR imaging.** *Radiology* 2012;262:206–15
25. Walsh AJ, Wilman AH. **Susceptibility phase imaging with comparison to R2 mapping of iron-rich deep grey matter.** *Neuroimage* 2011;57:452–61
26. Liem MK, Lesnik Oberstein SA, Versluis MJ, et al. **7 T MRI reveals diffuse iron deposition in putamen and caudate nucleus in CADASIL.** *J Neurol Neurosurg Psychiatry* 2012;83:1180–85
27. Schweser F, Deistung A, Lehr BW, et al. **Quantitative imaging of intrinsic magnetic tissue properties using MRI signal phase: an approach to in vivo brain iron metabolism?** *Neuroimage* 2011;54:2789–807
28. Patenaude B, Smith S, Kennedy D, et al. **A Bayesian model of shape and appearance for subcortical brain segmentation.** *Neuroimage* 2011;56:907–22
29. Batista S, Zivadinov R, Hoogs M, et al. **Basal ganglia, thalamus and neocortical atrophy predicting slowed cognitive processing in multiple sclerosis.** *J Neurol* 2012;259:139–46
30. Habib CA, Liu M, Bawany N, et al. **Assessing abnormal iron content in the deep gray matter of patients with multiple sclerosis versus healthy controls.** *AJNR Am J Neuroradiol* 2012;33:252–58
31. Zivadinov R, Weinstock-Guttman B, Benedict R, et al. **Preservation of gray matter volume in multiple sclerosis patients with the Met allele of the rs6265 (Val66Met) SNP of brain-derived neurotrophic factor.** *Hum Mol Genet* 2007;16:2659–68
32. Benjamini Y, Hochberg Y. **Controlling the false discovery rate: a practical and powerful approach to multiple testing.** *J R Stat Soc Series B-Methodological* 1995;57:289–300
33. Martin WR, Ye FQ, Allen PS. **Increasing striatal iron content associated with normal aging.** *Mov Disord* 1998;13:281–86
34. Zacharski LR, Ornstein DL, Woloshin S, et al. **Association of age, sex, and race with body iron stores in adults: analysis of NHANES III data.** *Am Heart J Jul* 2000;140:98–104
35. Milman N. **Serum ferritin in Danes: studies of iron status from infancy to old age, during blood donation and pregnancy.** *Int J Hematol* 1996;63:103–35
36. Youdim MB, Ben-Shachar D, Yehuda S. **Putative biological mechanisms of the effect of iron deficiency on brain biochemistry and behavior.** *Am J Clin Nutr* 1989;50(3 Suppl):607–15
37. Rouault TA, Zhang DL, Jeong SY. **Brain iron homeostasis, the choroid plexus, and localization of iron transport proteins.** *Metab Brain Dis* 2009;24:673–84

38. Langkammer C, Krebs N, Goessler W, et al. **Susceptibility induced gray-white matter MRI contrast in the human brain.** *Neuroimage* 2012;59:1413–19
39. Wu Z, Mittal S, Kish K, et al. **Identification of calcification with MRI using susceptibility-weighted imaging: a case study.** *J Magn Reson Imaging* 2009;29:177–82
40. Haacke EM, Miao Y, Liu M, et al. **Correlation of putative iron content as represented by changes in R2* and phase with age in deep gray matter of healthy adults.** *J Magn Reson Imaging* 2010;32:561–76
41. Cherubini A, Peran P, Caltagirone C, et al. **Aging of subcortical nuclei: microstructural, mineralization and atrophy modifications measured in vivo using MRI.** *Neuroimage* 2009;48:29–36
42. Stein T, Moritz C, Quigley M, et al. **Functional connectivity in the thalamus and hippocampus studied with functional MR imaging.** *AJNR Am J Neuroradiol* 2000;21:1397–401
43. Herrero MT, Barcia C, Navarro JM. **Functional anatomy of thalamus and basal ganglia.** *Childs Nerv Syst* 2002;18:386–404
44. Schenck JF, Zimmerman EA. **High-field magnetic resonance imaging of brain iron: birth of a biomarker?** *NMR Biomed* 2004; 17:433–45
45. Langkammer C, Krebs N, Goessler W, et al. **Quantitative MR imaging of brain iron: a postmortem validation study.** *Radiology* 2010;257:455–62
46. Zecca L, Youdim MB, Riederer P, et al. **Iron, brain ageing and neurodegenerative disorders.** *Nat Rev Neurosci* 2004;5:863–73